Journal of the European Ceramic Society 20 (2000) 851–858

In situ evaluation of dimensional variations during water extraction from alumina injection-moulded parts

Wei-Wen Yang*, Min-Hsiung Hon

Department of Materials Science and Engineering, National Cheng Kung University, Tainan, Taiwan, ROC

Received 10 May 1999; received in revised form 22 July 1999; accepted 8 August 1999

Abstract

The dimensional variations of alumina injection-moulded compacts containing polyethylene glycol (PEG) binders during solvent debinding were studied. A dilatometer was set up for monitoring the length changes of compacts in situ. The results indicate that the parts expanded dramatically as soon as they came into contact with preheated water. After the initial sharp expansion, moulded compacts swelled slowly and reached the maximum expansion. The dimensions of specimen then maintained at a fixed value and the parts finally shrank drastically when water was drained out. Based on the results obtained, the causes of length changes for specimens immersed in water are discussed. In addition, the effects of debinding temperature and molecular weight of PEG on the length changes of specimens were also examined.

Keywords: Al_2O_3; Debinding; Dimensional change; Injection moulding

1. Introduction

In recent years, powder injection moulding (PIM) has been recognized as a cost-effective process for the production of relatively small, high performance and complex shaped ceramics, metals in massive form.[1–4] The method usually includes the following major steps: mixing of powder with the binder system, moulding, debinding and sintering.[5,6]

Historically, removal of the binder from the shaped powder compact has been considered the most critical step in the PIM process because of the long time needed to burn out the binders without introducing defects. It is the source of great difficulties and is often the manufacturing step that is least understood.

Among the debinding methods, thermal debinding was the first process developed and is still widely used in the PIM industry because of its simplicity and the low equipment investment.[7,8] However, the process is time-consuming because the debinding rate must be slow in order to avoid internal pressure buildup from decomposed gas, which causes cracking, blistering and exfoliation during debinding.[9–12]

In order to overcome these problems in thermal debinding, solvent debinding[13,14] has been widely accepted by the industry, because as it replaces thermal debinding, only small changes in binder design combined with a small equipment investment are required. In the solvent debinding process, a portion of the binder can be chemically removed by using solvents like acetone, trichloroethane or heptane, thus creating continuous pore channels throughout the part. Once continuous porosity has been created, the subsequent thermal cycle can be as short as 3 or 4 hours.

Although solvent extraction is probably the fastest debinding route, a problem with solvent debinding concerns the nature of common solvents; the organic solvents most adopted in solvent debinding now are flammable, carcinogenic and not environmentally acceptable. In addition, several types of defects could still occur during the solvent debinding step. These defects are mainly caused by the large dimensional changes when parts are immersed in the solvent, especially for organic solvents.[7,15] The sharp increase and decrease in dimension certainly results in significant stresses in specimens.

For eliminating the use of unsound solvents, water-soluble polyethylene glycols (PEGs) are used in this study to modify the pattern of debinding in ceramic injection molding. As PEGs are very safe chemicals and

* Corresponding author.

0955-2219/00/$ - see front matter
PII: S0955-2219(99)00221-6

are used quite extensively in the food industry, permission was obtained from the local water authorities to dump the water/PEG containing solvents into the drain after debinding.

Considerable efforts have been made to understand the transport of binder vapor and fluid in the moulded compact during solvent debinding and thermal debinding.[11,16–20] None of these studies, however, has considered the debinding mechanism and the dimensional variations for PIM specimens during solvent debinding based on water extraction. Solubility relations in a polymer system are more complex than those among low-molecular-weight compounds, it occurs when the free energy of mixing $\Delta G_{mix} = \Delta H_{mix} - T\Delta S_{mix}$ is negative. It is clear that the topology of the polymer is highly important in determining its solubility. Cross-linked and crystalline polymers do not dissolve but only swell if indeed they interact with the solvent at all. In part, at least, the degree of this interaction is determined by the extent of cross-linking and crystallinity.[21]

In solution, a polymer molecule is a randomly coiling mass most of whose conformations occupy many times the volume of its segment alone. The size of the molecular coil is very much influenced by the polymer-solvent interaction forces. In a thermodynamically "good" solvent, where polymer-solvent contacts are highly favored ($\Delta G_{mix} < 0$), the coils are relatively extended. In a "poor" solvent ($\Delta G_{mix} > 0$), they are relatively contracted. In a sufficiently poor solvent, or at a sufficiently low temperature, it is possible to achieve the condition ($\Delta G_{mix} = 0$) where the chain attains its unperturbed dimensions. This special point is called the Flory temperature θ, at which segment–segment and segment–solvent attractive and repulsive forces compensate. A solvent used at $T = \theta$ is called a theta solvent. At a temperature below the theta temperature, the solvent becomes a poor solvent and at a temperature above theta temperature, a good solvent.

The main objective of this research lies in evaluating the dimensional variations of water-extracted alumina injection-moulded parts in situ. Based on these results, the causes of length changes for specimens immersed in water will be discussed. Moreover, if the mechanisms that cause dimensional variation during solvent debinding are understood, steps may be taken to minimize the defects.

2. Experimental procedure

Commercial purity powder (Japan, Showa Denko, AL-160-SG4) was used in the study. The average particle size was 0.6μm and specific surface area was 4.1 cm^2/g.

A multi-component binder system was used to prepare the alumina feedstock. The binders used in the experiment are listed in Table 1. For these binders, the major portion consisted of PEG4000, the backbone consisted of polyethylene wax (PE wax) for good strength during debinding, and stearic acid (SA) was used for improving flowability. The total alumina powder content was 55 vol%, and the remaining 45 vol% consisted of the aforementioned polymers with a weight ratio of PEG4000: PE wax: SA = 65:30:5.

To understand the effect of molecular weight on debinding, PEG1500 and polyethylene oxide (PEO4000 k) were used respectively to substitute for PEG4 k as the major binder. The melting points of the binders were determined from differential scanning calorimeter (DSC) curves obtained by a Du Pont 910 analyzer. Table 2 illustrates the compositions of binder systems used in the study. Three feedstocks were prepared by using a sigma-type blade kneader having a rotation frequency of 50 r.p.m. The alumina powder was initially added into the kneader and preheated at 100°C for 30 min in order to achieve the temperature distribution. The binders were subsequently added and mixed for 90 min. Granules were obtained by continuously rotating the blade during cooling from 100 to 50°C.

The feedstock was then transferred to an 80 tonne (clamp capacity) injection-moulding machine where rectangular test bars with dimensions of 75×5×4 mm were moulded. The barrel temperature ranged from 100 to 120°C depending on the binders used in the feedstock. The mould temperature was maintained at 40°C.

A dilatometer was designed for monitoring the length changes of compacts in situ, as shown in Fig. 1. In this set-up, a thermocouple was employed for recording the temperature variation of the specimen during solvent debinding. The alumina injection moulded compact was fixed at one end and came into contact with the dilatometer directly at the other end. The weight of the graphite push rod, as indicated in Fig. 1, was offset by the microbalance. To simulate the case where the moulded

Table 1
Binders used in the experiment

Binder	Source	Density (g/cm^3)
PEG1500	Merck, Germany	1.17
PEG4000	Merck, Germany	1.22
PEO4000 K	Merck, Germany	1.21
Polythene wax	Allied	0.94
Stearic acid	Merck, Germany	0.94

Table 2
The compositions of binder system employed in the study

Samples	PEG1500	PEG4000	PEO4000 k	PE wax	SA
Weight percentage (%)					
A	65			30	5
B		65		30	5
C			65	30	5

parts were immersed into a preheated water bath, water was preheated in a water container. Once the temperature of the water was stable, the preheated water was introduced into the isothermal sample tank. The length changes of the specimens were measured by the dilatometer as the solvent debinding proceeded. When it was terminated, the water was drained to simulate the lifting of parts out of the solvent bath in real practice.

For direct observations of the pore structure, a scanning electron microscope (SEM) was used to analyze the fracture surface of specimens after being debound for different periods of time.

3. Results and discussion

Fig. 2 shows the length and temperature changes of alumina specimens after being immersed in water at 50°C for different periods of time. The curve of dimension could be divided into four stages. In the first stage, the parts expanded drastically as soon as they came into contact with the preheated water. After the initial sharp expansion, moulded compacts expanded slowly and reached a total expansion of about 0.27% after 1.5 h. The dimension of the specimen was unchanged in the third stage. Finally, the parts shrank drastically when water was drained out.

The sharp dimensional changes that occurred when the water was introduced into or drained from the sample tank corresponded with the temperature change, as shown in Fig. 2. The sharp increase and decrease at the beginning and the end of debinding can be assumed to result from thermal expansion. This hypothesis was confirmed by the experimental result in which the compact was immersed in water at room temperature, as shown in Fig. 3. With no temperature difference between the specimen and water, the sharp dimensional changes did not occur when water was introduced into and drained out from the sample tank.

In contrast to the thermal expansion in the first stage, the cause of slow expansion in the second stage should be related to the debinding process. It has been postulated that dissolution of the binder is a slow process that occurs in two stages.[21] First, solvent molecules slowly diffuse into the binder to produce a swollen gel. If the molecular interaction is large because of cross-linking, crystallinity, or strong hydrogen bonding, then swelling of the binder results. If the attraction between the polymer and solvent is larger than the interaction between polymers, then the second stage of binder dissolution

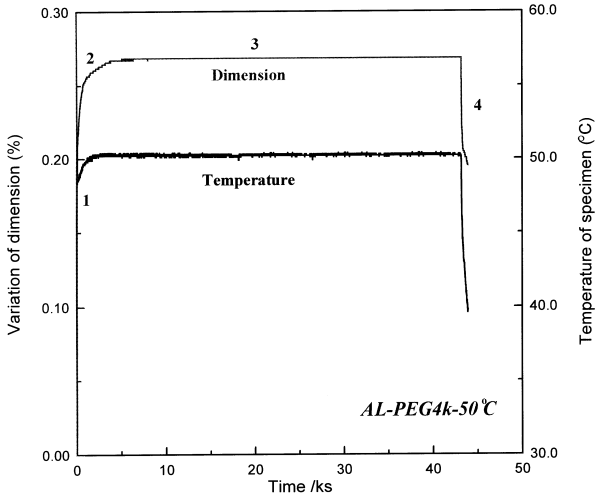

Fig. 2. The length changes of alumina specimen after being immersed in water at 50°C for different periods of time.

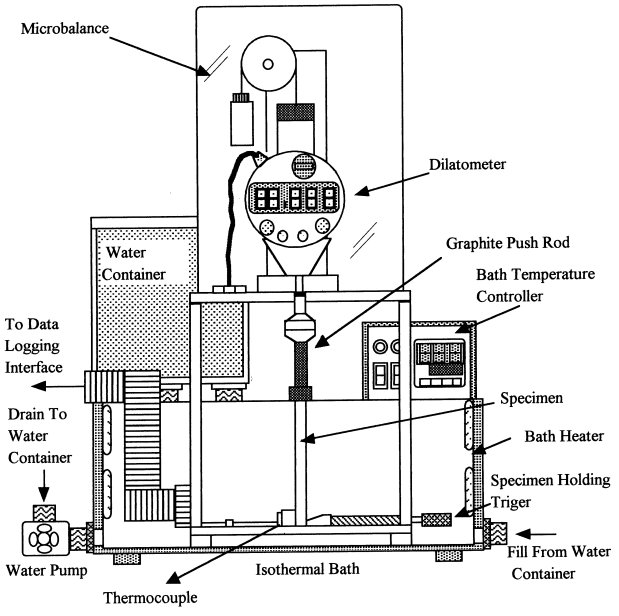

Fig. 1. The set-up of the dilatometer for measuring length changes of specimens during solvent debinding.

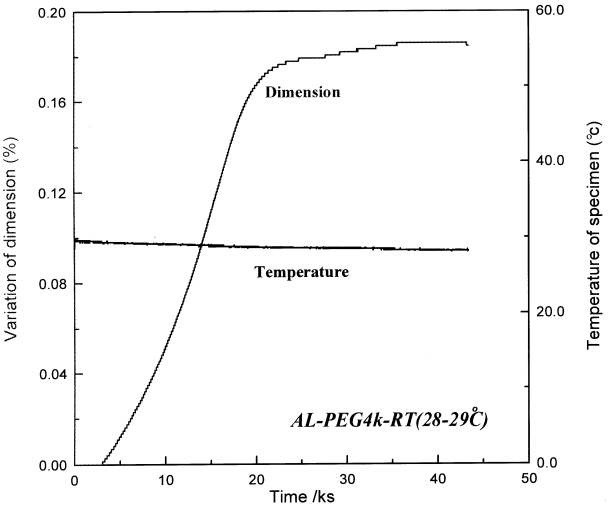

Fig. 3. The length changes of alumina specimens after being immersed in water at room temperature for different periods of time.

can take place. Here, the gel gradually disintegrates into a true solution.

The binder system used in the experiment is composed of PEG4000, PE wax and SA. The effect of SA was ignored because the quantity of SA is very small. Fig. 4 shows the length changes of the pure PE wax specimens after being immersed in water, ranging from room temperature to 50°C. It is seen that excepting thermal expansion, there was no swelling.

The nature of water association with PEGs has been widely accounted for in a very large portion of researches.[22–27] The existing literature is confusing as there is mention of mono-, di-, tri-, tetra- and hexahydrates. On first consideration it appears that the most probable associations of PEGs with water would be as either mono- or dihydrates, as it is only possible to hydrogen-bond one or two water molecules to the ether group of the polymer. No matter what kind of hydrated complexes are formed, all these studies indicate that the PEGs would swell in water. The expansion in the second stage, therefore, must have been due to the interaction between PEG and water.

This deduction was confirmed by the length changes of alumina specimen after being debound in water at 40°C for different periods of time, as shown in Fig. 5. The dimensional variation as indicated in Fig. 5, reached a stable value after being debound for 3.5 h. Direct observations were made on binder distribution and pore evolution by SEM so as to verify the information obtained from the dilatometer. Different areas, including the outer edges and the centre regions of fractured samples were examined. Figs. 6 and 7 show, respectively, the morphology of the outer edge and centre of samples after they were debound in the water bath at 40°C for different periods of time. For 5-min solvent-debound parts, the morphology at the outer edge, as shown in Fig. 6(b), demonstrated that pores with different sizes were formed. Some were inter-particle pores and some were within the binders, indicating that the three binder components had mixed and the soluble binder (PEG) had been extracted. After being debound for 1 h, most of the PEG was removed, leaving the insoluble binders in the contact region, as shown in Fig. 6(d).

Similar examinations were also made at the centre region of fractured specimens. Fig. 7(b) shows that there were still no pores generated in the centre of the specimen after being debound for 2 h, indicating that the PEG did not dissolve at this time. Some pores were not observed in the centre region until the end of 3 h of debinding, as demonstrated in Fig. 7(c). The consequences indicate that the PEG dissolution started from the surface and progressed toward the centre of the specimen, and 3–4 hours are needed for water molecules to penetrate into the centre of the specimen and interact with the all PEG molecules. It matches the time for specimen reaching a stable dimension during solvent debinding, as shown in Fig. 5.

According the above results, the length changes during the second and third stages can be summarized as follows.

As the debinding proceeds, water diffuses into the specimen from the surface and progresses toward the centre of the compact. The PEG swells to gradually form a gel when in contact with water, causing the specimen to expand. When water molecules penetrate into the centre of specimen, interconnected pore channels are formed from exterior to interior and serve as a conduit to drain the swollen solution. Moreover, all the PEG molecules have come into contact with water molecules by this time. Once the equilibrium between PEG and

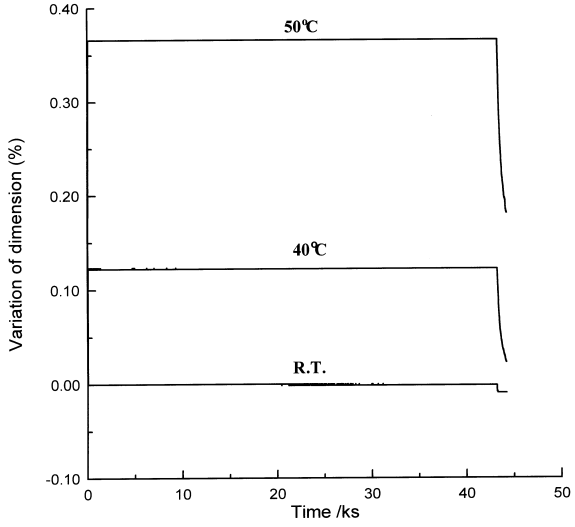

Fig. 4. The length changes of pure polyethylene wax specimens after being immersed in water for different periods of time at different temperatures.

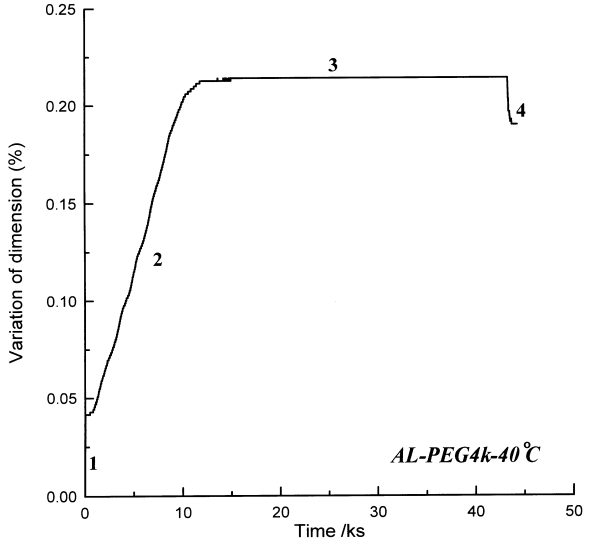

Fig. 5. The length changes of alumina specimens after being immersed in water at 40°C for different periods of time.

water is reached, the dimensional variation of specimen reaches the maximum value and remains fixed.

Fig. 8 illustrates the effect of water temperature on the length changes of alumina specimens with PEG4000 after being debound for different periods of time. As expected, a higher temperature results in a larger thermal expansion in the first stage. In addition, the solubility of PEG increases with the debinding temperature, which leads to a higher penetrated rate for water, therefore, the time needed for PEG molecules to interact

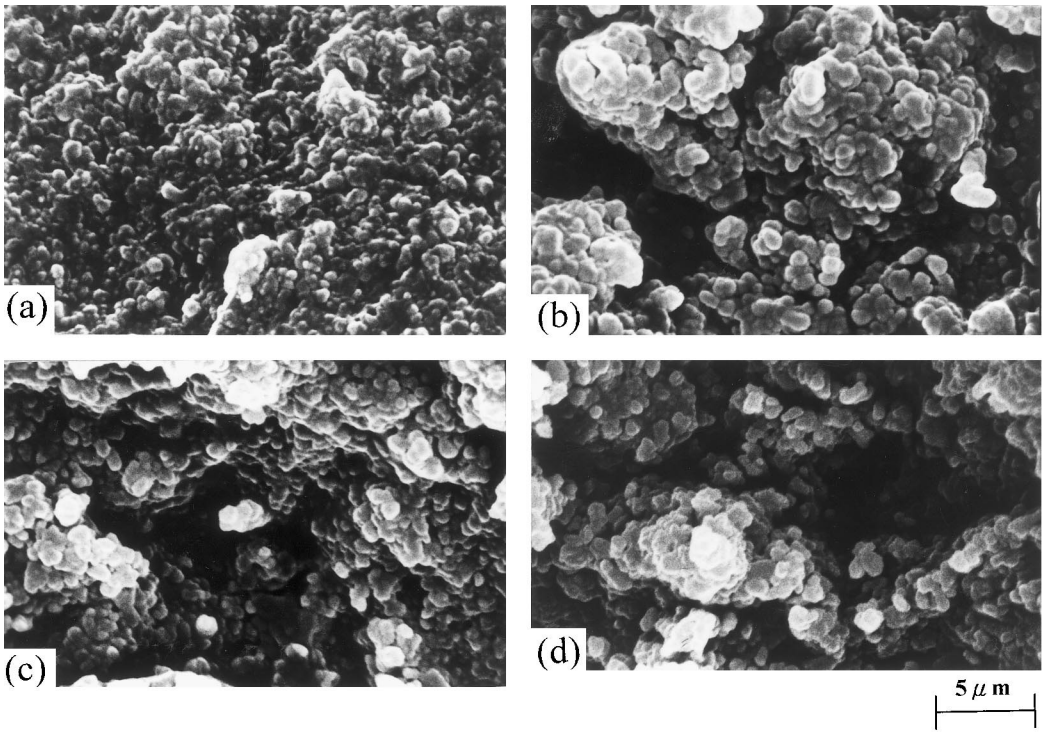

Fig. 6. SEM morphology of cross-section near the edge for samples (a) as-moulded (b)(c)(d) debound at 40°C for 5, 30 and 60 min respectively.

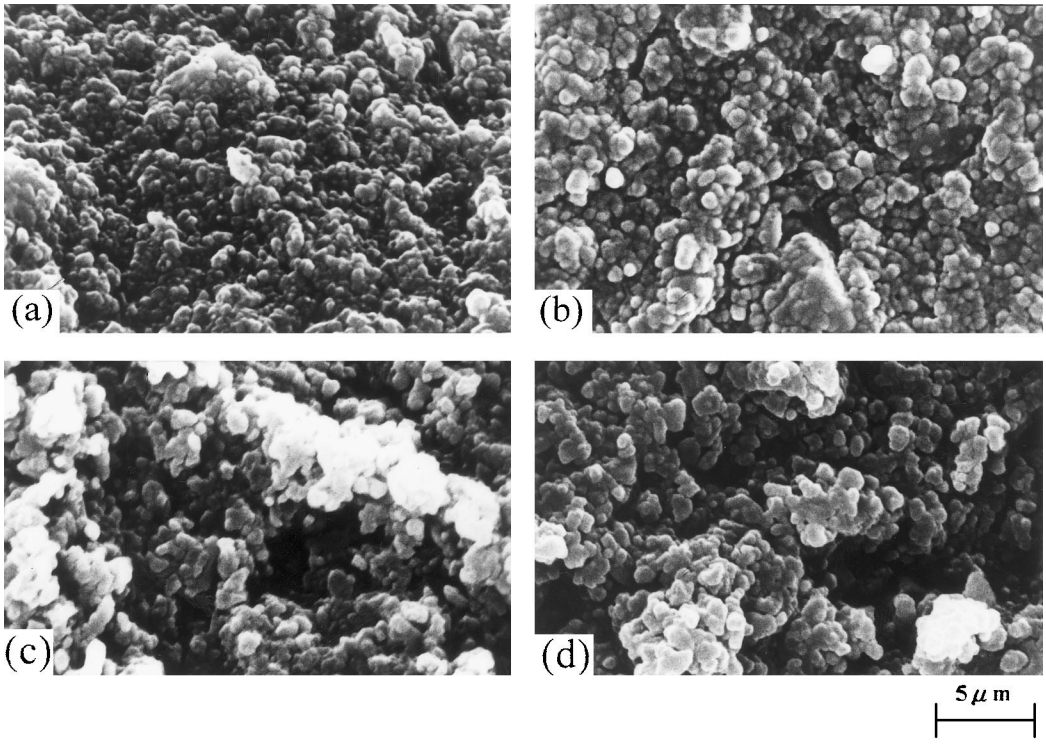

Fig. 7. SEM morphology of cross-section near the center for samples (a) as-moulded (b)(c)(d) debound at 40°C for 2, 3 and 4 h respectively.

fully with water molecules was shortened. The length of specimen consequently could reach a stable length in a shorter time at a higher temperature.

Moreover, Fig. 8 also shows that the higher the temperature of water, the smaller is the length change in the second stage. The results imply that the extent of swelling of PEG decreases as the water temperature increases because the expansion in the second stage was due to the swelling of PEG.

In fact, the state of association of PEG with water has been clearly indicated in previous studies[23] to be very temperature dependent and reveals a marked decrease in swelling as the temperature was increased. This is because the net entropy change is negative when the dry PEG is dissolved in water.[23] The term $-T\Delta S_{mix}$ in the equation $\Delta G_{mix} = \Delta H_{mix} - T\Delta S_{mix}$ has a positive value which increases with temperature and, therefore, raises the free energy of mixing as the temperature rises. The consequence is a decrease in the degree of swelling at higher temperatures.

In addition, it is worth noting the dimensional variation of a specimen debound at 55°C as shown in Fig. 8. No swelling occurred excepting thermal expansion, as exhibited in this curve. The experiment was repeated several times and the results were almost the same. Fig. 9 illustrates the effect of water temperature on the length changes of alumina specimens with PEG1500. It reveals that the specimen did not expand at 45°C excepting the initial thermal expansion. It is interesting to find out that the extent of dilation for the specimen at 40°C is higher than that at 45°C even though the thermal expansion is smaller at 40°C. The results imply that there may be another cause for the disappearance of swelling. It could be related to the properties of the binders used in the experiment.

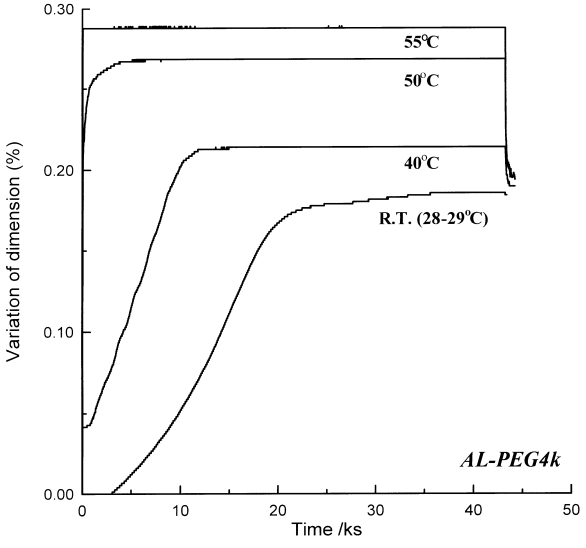

Fig. 8. The effect of water temperature on the length changes of alumina specimens with PEG4000 during solvent debinding.

This was confirmed by further DSC analysis, as shown in Fig. 10. The DSC analysis indicated that the melting points of PEG4000 and PEG1500 are 54.3 and 43.8°C respectively. The presence of crystallinity may give rise to sufficiently high intermolecular forces to prevent solubility; this may result in the increase of dilation. When the temperature approaches the melting point, the crystallinity decreases and the solubility can be easily achieved; this may decrease the extent of dilation. The above evidences suggest that the disappearance of swelling in the second stage is a consequence of the melting of PEG.

Moreover, Fig. 10 also shows that the melting point of crystalline PEO4000 k is about 64.8°C. The effect of water temperature on the length changes of alumina specimens with PEO4000 k is shown in Fig. 11. The

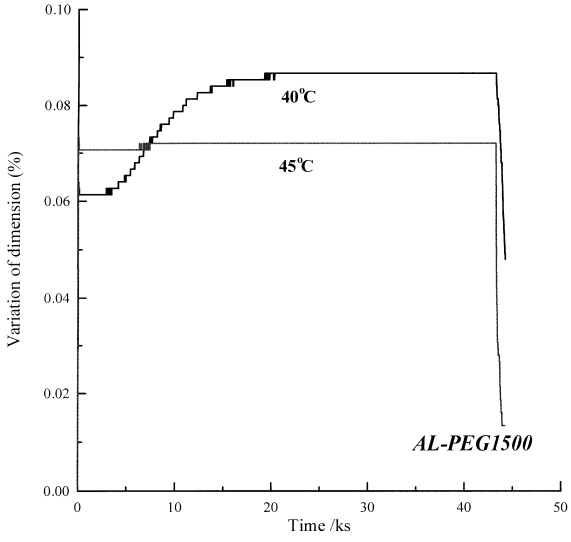

Fig. 9. The effect of water temperature on the length changes of alumina specimens with PEG1500 during solvent debinding.

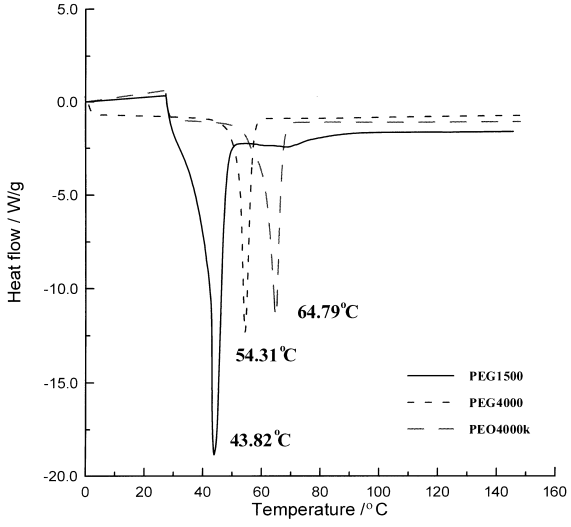

Fig. 10. The differential scanning calorimetric curves of PEG1500, PEG4000, and PEO4000 k.

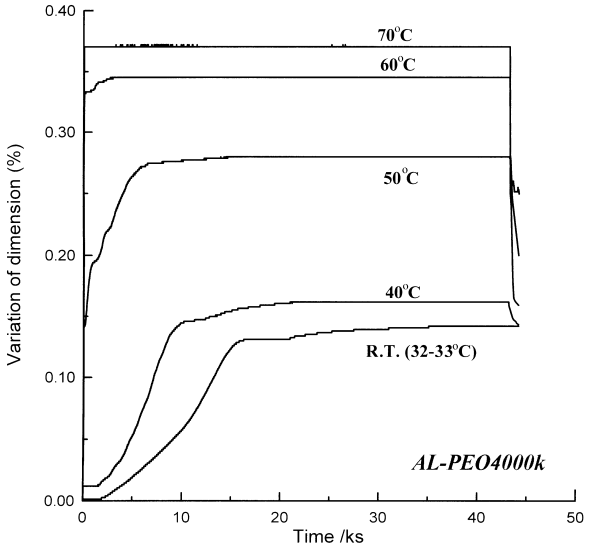

Fig. 11. The effect of water temperature on the length changes of alumina specimens with PEO4000 k during solvent debinding.

trend of length changes is similar to the specimens with PEG4000. However, a little swelling still occurred for specimens with PEO4000 k at 60°C. The swelling in the second stage did not disappear until the water temperature reached 70°C, which matches our deductions. Once the water temperature exceeded the melting point of PEGs, the swelling curve in the second stage disappeared as a result of the melting of PEGs.

4. Conclusions

The dimensional variations of alumina injection-moulded compacts containing PEG binders during solvent debinding have been studied in this paper. Initially, owing to the temperature differences between parts and preheated water, parts expanded drastically as soon as the parts came into contact with preheated water. As the debinding proceeded, water diffused into the specimen from the surface and progresses toward the centre of the compact. The PEG swelled to gradually form a gel when in contact with water, causing the specimen to expand. When water molecules penetrate into the centre of specimen, all the PEG molecules have came into contact with water molecules. Once the equilibrium between PEG and water was reached, the dimensional variation of specimens reached the maximum value and remained fixed. Finally, the specimen shrank drastically when water drained out.

The extent of thermal expansion and solubility of PEG increased with the debinding temperature, which lead to a higher penetration rate of water molecules, shortening the time needed for PEG molecules to interact fully with water. The length of the specimen consequently became stable in a shorter time at a higher temperature.

When the temperature approached the melting point of PEGs, the crystallinity decreased and the solubility was easily achieved, which decreased the extent of dilation. Once the water temperature exceeded the melting point of PEGs, the swelling curve in the second stage disappeared as a result of the melting of PEGs.

Acknowledgements

The authors wish to thank the National Science Council of the ROC for their support of this work under the project (NSC-87-2216-E-006-042).

References

1. Takekawa, J., Effect of binder composition on debinding and sintering process of injection moulded Fe-8Ni mixed powders. *J. Mater. Res.*, 1996, **11**, 1127–1136.
2. Juang, H. Y. and Hon, M. H., The effect of calcination temperature on the behaviour of HA powder for injection moulding. *Ceram. Inter.*, 1997, **23**, 383–387.
3. de With, G. and Witbreuk, P. N. M., Injection moulding of zirconia (Y-TZP) ceramics. *J. Eur. Ceram. Soc.*, 1993, **12**, 343–351.
4. Zhang, T., Evans, J. R. G. and Woodthorpe, J., Injection moulding of silicon carbide using an organic vehicle based on a preceramic polymer. *J. Eur. Ceram. Soc.*, 1995, **15**, 729–734.
5. Hunold, K., Greim, J. and Lipp, A., Injection moulded ceramic rotors-comparison of SiC and Si_3N_4. *Powder Met. Int.*, 1989, **21**, 17–23.
6. Edirisinghe, M. J. and Evans, J. R. G., Systematic development of the ceramic injection molding process. *Mater. Sci. Eng.*, 1989, **A109**, 17–26.
7. German, R.M. *Powder Injection Molding*, Metal Powder Industries Federation Princeton, NJ, USA, 1990, pp. 321–334.
8. Wiech, Jr., R. E., Method for removing binder from a green body. US Patent 4404166, 13 September 1983.
9. Bandyopadhyay, G. and French, K. W., Injection molded ceramics: critical aspects of the binder removal process and component fabrication. *J. Eur. Ceram. Soc.*, 1993, **11**, 23–34.
10. Hwang, K. S. and Tsou, T. H., Thermal debinding of powder injection molded parts: observations and mechanisms. *Metall Trans. A*, 1992, **23A**, 2775–2782.
11. Verweij, H. and Bruggink, W. H. M., Reaction-controlled binder burnout of ceramic multilayer capacitors. *J. Am. Ceram. Soc.*, 1990, **73**, 226–231.
12. Woodthorpe, J., Edirisinghe, M. J. and Evans, J. R. G., Properties of ceramic injection moulding formulations. Part 3: polymer removal. *J. Mater. Sci.*, 1989, **24**, 1038–1048.
13. Johnson, K. P., Process for fabricating parts from particulate material. US Patent 4765950, 23 August 1988.
14. Wiech, Jr., R. E., Manufacture of parts from particulate material. US Patent 4197118, 8 April 1983.
15. Amaya, H. E., Solvent dewaxing: principles application. *Proceedings of the Powder Metallurgy Conference Advances in Powder Metallurgy*, 1990, **3**, 233–246.
16. Shaw, H. M. and Edirisinghe, M. J., Porosity development during removal of organic vehicle from ceramic injection mouldings. *J. Eur. Ceram. Soc.*, 1994, **13**, 135–142.
17. Shaw, H. M. and Edirisinghe, M. J., Shrinkage and particle packing during removal of organic vehicle from ceramic injection mouldings. *J. Eur. Ceram. Soc.*, 1995, **15**, 109–116.
18. Lograsso, B. K. and German, R. M., Thermal debinding of injection moulded powder compacts. *Powder Metall. Int.*, 1990, **22**, 17–22.

19. Calvert, P. and Cima, M., Theoretical models for binder burnout. *J. Am. Ceram. Soc.*, 1990, **73**, 575–579.
20. Tsai, D. S. and Chen, W. W., Solvent debinding kinetics of alumina green bodies by powder injection moulding. *Ceram. Inter.*, 1995, **21**, 257–264.
21. Billmeyer, Jr., F. W., *Textbook of Polymer Science*, John Wiley and Sons, New York, 1984, 2nd ed., p. 23.
22. Kjellander, R. and Florin, E., Water structure and changes in thermal stability of the system Poly(ethylene oxide)-water. *J. Chem. Soc., Faraday Trans. 1*, 1981, **77**, 2053–2077.
23. Graham, N. B., Nwachuku, N. E. and Walsh, D. J., Interaction of poly(ethylene oxide) with solvents: 1. Preparation and swelling of a crosslinked poly(ethylene oxide) hydrogel. *Polymer*, 1982, **23**, 1345–1349.
24. Graham, N. B., Zulfiqar, M. N., Nwachuku, E. and Rashid, A., Interaction of poly(ethylene oxide) with solvents: 4. Interaction of water with poly(ethylene oxide) crosslinked hydrogels. *Polymer*, 1990, **31**, 909–916.
25. Ishidao, T., Akagi, M., Sugimoto, H., Onoue, Y., Ikai, Y. and Arai, Y., Swelling equilibria of poly(*N*-isopropylacrylamide) gel in aqueous polymer solutions. *Fluid Phase Equilibria*, 1995, **104**, 119–129.
26. Keys, K. B., Andreopoulous, F. M. and Peppas, N. A., Poly(-ethylene glycol) star polymer hydrogels. *Macromolecules*, 1998, **31**, 8149–8156.
27. Gayet, J.-Ch., He, P. and Fortier, G., Bioartificial polymeric material: Poly(ethylene glycol) crosslinked with albumin. *J. Bioactive Compat. Poly.*, 1998, **13**, 179–197.